Robotica (2016) volume 34, pp. 1128–1150. © Cambridge University Press 2014
doi:10.1017/S0263574714002100

Time-variant artificial potential field (TAPF): a breakthrough in power-optimized motion planning of autonomous space mobile robots

Matin Macktoobian* and Mahdi Aliyari Shoorehdeli

Fault Detection and Identification Lab (FDI), Electrical and Computer Engineering Faculty, K. N. Toosi University of Technology, Tehran, Iran

(Accepted July 16, 2014. First published online: August 15, 2014)

SUMMARY

In this paper, a novel scheme is presented to conquer the motion-planning problem for autonomous space robots. Minimizing the consumed energy of atomic batteries within the daily planetary missions of robot on the planet is taken into account, i.e., utilization of the generated solar power by its embedded photocells leads to saving energy of batteries for night missions. Aforementioned objective could be acquired by appropriate interaction of motion planning paradigm with shadows of obstacles. Modeling of the shadow with the proposed artificial potential field leads to generalize the concept of potential fields not only for static and dynamic obstacles but also for being confronted with the intrinsic time-variant phenomena such as shadows. With due attention to the noticeable computational complexity of the introduced strategy, fuzzy techniques are applied to optimize the sampling times effectively. To accomplish this objective, a smart control scheme based on the fuzzy logic is mounted to the primitive version of algorithm. Regarding the need to identify some structural parameters of obstacles, PIONEER^{TM} mobile robot is designed as a test bed for the verification of simulated results. Investigation on empirical accomplishments shows that the goal-oriented definition of Time–Variant Artificial Potential Fields is able to resolve the motion-planning problem in planetary applications.

KEYWORDS: Artificial potential field; Motion planning; Mobile robot; Navigation; Space Robotics.

1. Introduction

Special attention to the motion-planning problem has been rather accompanied with seminal primary innovations in the territory of mobile robots. Various applications of these creatures in both industrial utilizations and some aspects of daily life have led to emerge successive struggles among researchers. As a sequel, design of efficient approaches for the navigation of mobile robots in different environments with various operational circumstances are taken into account. Various strategies have stemmed from different attitudes of roboticians upon the motion-planning problem and the novel illustrations used to define and resolve it. Obviously, technological achievements could provide appropriate beds to develop and transition them from subjective concepts into empirical realities. A great deal of endeavors to encounter with motion planning problem are beholden of successive researches by computer science researchers in over half a century. Emersion of artificial intelligence and its advanced algorithms, which could be utilized to model maps and terrains with graphs and trees, allows us to generate a series of smart schemes for this problem. Koenig and Likhachev[1] tried to solve motion planning problem among static obstacles. Partially known environments make the planner compute the best route within the process of map completion for several times in order to acquire the optimized one. Result of such attempts led to the advancement of the latter approach by stents.[2] Progressive distributions of D^* algorithm such as D^*Lite,[3] focused D^{*4} and $FieldD^*$,[5] and

* Corresponding author. E-mail: matinking@hotmail.com

*TWD**[6] are evolved to provide some improvements such as more simplicity and higher efficiency. In spite of all achievements, which could be acquired with the utilization of AI-based techniques, there are some considerable drawbacks for the implementation of these in real problems. On one hand, the existence of circumferential map could be considered as a necessary condition to partition the problem into graph form; with due attention to most of real-time problems without complete knowledge about the environment and noticeable computational complexity of AI-based algorithms, planner must run these sophisticated algorithms over and over again to evaluate the new path based on the updated map which could make some problems for robots to use these approaches practically. On the other hand, it is possible to confront with some special situations which may not be modeled by above schemes as precise as the planner needs. Reaching into both robust navigation of mobile robots and simple empirical implementation is stemmed from the advent of artificial potential fields (APF). More ever, we are prone to show that computational efficiency of our strategy might acquire noticeable advantages in comparison with AI-based approaches just like A^* technique and its predecessors in the perspective of the elimination of recursive procedures within computational processes. One might take into account the necessity of huge data structures to not only compute the potential elite paths but also compare all heuristic candidates for the best route as a drawback in the perspective of both timing and space computational complexity. It should be stressed upon that this problem will be more challenging in case of fully explorative missions, where planning of efficient heuristic data will rather be impossible. Instead, our straightforward scheme is entirely devoid of recursive procedures and the computation of APF within each time slot will be considered as a numerical control signal to drive robot independently.

Attention to obstacle avoidance for both manipulators and mobile robots in the perspective of real-time attitude is studied by Khatib.[7] Given the extent of attractive and repulsive potentials which were applied virtually to robot, obstacles, and target, APF idea transformed to one of the pioneer strategies to solve motion planning problem in the vast territory of mobile robotics. Oscillation of a robot due to the utilization of simple repelling functions could be taken into account as a field of research. Furthermore, with due attention to weak operation of classical APFs near the target, mounting of rotational forces to acquire smoother trajectories are studied in ref. [8]. Considering dynamic obstacles, the path-planning problem will change into a challenging stuff, needing advanced distributions of APFs.[9,10] Investigation of resolving of local minima problem over three decades depicts it as one of the main drawbacks of primary APFs, and a great deal of strategies are proposed to prevail over this important problem. Local minima inhibition by simulation annealing optimization (SAO) could be mentioned as an improving scheme, which is tested empirically on a snake robot as a test bed.[11] Fragile efficiency of SAO in complex environments led to the utilization of memory modules to record various states of robot related to the target. This idea can not only reach into the objective but is also capable of applying some improvements to the attenuation of robot oscillations within the navigation process.[12] Particle swarm optimization under a quantum attitude[13] may lead to some progressions on the real-time control of a robot. Velocity dipole fields[14] could be used in real-time missions, as well. A recent work, which could be categorized in real-time applications, is discussed in ref. [15]. Improvements to some specified local minima problems by route planning are investigated in ref. [16]. Considering the effective role of GA algorithms in optimization problems, some researchers have applied this type of optimization technique for resolving the local minima problem,[17] whereas formal utilization of GA algorithms in mobile robotics could be referred to utilization of evolutionary APFs[18] on smooth rotational movements of a robot in the vicinity of obstacles. Study on multi-robot systems as a seminal concept for the evolution of swarm robotics to plan interaction of robots together could be classified into various subjects such as management of collision detection among robots. Proposition of dynamic APF[19] is due to acquisition of an efficient tool for control of collision detection among agents by the introduction of a new repulsive potential term, whereas collision detection problem in view of obstacles could be resolved by traditional APFs. Velocity obstacle paradigm[20,21] is another well-known collision detection method that maps moving obstacles into a 2D velocity space.

Handling of the local minima problem in 3D motions may transform the straightforward APFs to the sophisticated ones. Furthermore, modeling of spatial obstacles by the implications of the control theory could be known as an innovation in this field. Receding horizon control[22] tries to resolve virtual disturbances within the navigation process in multi-UAV missions. Aforementioned aim could be gained by an additional control term. Navigation of UAVs under the consideration of constraints was

https://doi.org/10.1017/S0263574714002100 Published online by Cambridge University Press

investigated in ref. [23]. The idea of adaptive APF[24] has been also suggested for acquiring a level of efficient navigation for unmanned aircrafts in the presence of local minima traps. Syncretizing the APF concept with AI-based algorithms such as A^* is stemmed from noticeable complexity of navigation in 3D work spaces. Obviously, the capability of A^* algorithm in the navigation of robot from the perspective of static obstacles allows us design a peculiar version of APFs to resolve the local minima problem specifically, which was studied in detail in ref. [25].

Usual procedure in the definition of APF, which was primarily introduced in the aforementioned research, is based on two different potentials, each of which is responsible for one of the main desired effects of obstacles and free spaces on the behavior of navigation system, i.e., attractive and repulsive forces could be taken into account as smart approaches to manage the motion planning problem as a modular one. Obviously, effective control on either attractive or repulsive forces is stemmed from such applied modular attitude toward APFs. Definition of APFs based on the Panel theory could be considered as a turning point in the history of this concept, which is basically imported from hydrodynamics[26] and will be investigated at length in Section 2.

As previously stated, appropriate navigation of robots in different environments and under some specific operational restrictions just could be fulfilled by the utilization of specified APFs. One may discern some differences between the navigation of typical mobile robots on the usual terrains and the navigation of autonomous space robots and planetary rovers on the terrestrial masses such as planets and asteroids, i.e., noticeable slippage on the rock or soft soil bed of the planet, intensive variations in temperature, hard planar winds, and so on make the designer reconsider the motion planning problem. One of the most critical points in this area is optimization of the consumed power within the exploratory missions. Planetary rovers utilize two main resources of energy within their missions: mounted sheets of photocells and atomic batteries. Produced power of photocells is usually used within daily missions, and the utilization of atomic will be specified to the night missions where there is no sunlight. Obviously, worthwhile and restricted energy of batteries is essential to guarantee the motion of rover in the night. Usual obstacles on space masses have noticeable height and width. So the robot will consider itself in a virtual night situation in crossing the vast shadows of obstacles. With due attention to long-time missions of planetary rovers, which may exceed over several years, handling of entrance into shadows must be taken into account efficiently. In other words, the proposed navigation scheme should percept the shadow as a special time-variant obstacle.

In this research, a novel APF based on the panel theory is proposed in order to gain the above objective. Time-varying nature of the shadow inspires us to progress a time-variant version of APFs, the so-called TAPF.[27] TAPF interprets the shadow of each obstacle as a Gaussian surface, and the virtual flux crossing this surface could be translated as an artificial potential field corresponding to that shadow. Furthermore, sophisticated definition of TAPF should be handled to compute it just when it is necessary. Therefore, applied computational overhead inflicted to planner due to critical computational complexity of the suggested approach could be resolved, i.e., a smart fuzzy controller will be mounted into the heart of the planner to achieve this aim. Extraction of some circumferential parameters is essential to construct appropriate TAPF.[28] A pure practical discussion on the extraction of these and their evaluation will be tested on the PIONEER^{TM} mobile robot.

The rest of the paper is organized as follows: A brief review on the panel theory and the definition of the panel-based APFs are gathered in Section 2. Section 3 completely describes the mathematical foundation of the TAPF concept. The overall view on control of the whole navigation system, including traditional APF and TAPF, is analyzed in Section 4. Computational optimization of TAPF is discussed in Section 5. Practical implementation of the technique is investigated in Section 6 to take into account the circumferential perception of the environment to extract desired parameters for the computation of TAPF. Empirical denouements for the implementation of planned ideas for the evaluation of circumferential parameters are investigated in Section 7 to validate applied strategies. Concluding remarks and interesting themes stemmed from the proposed idea of this paper, which could be taken into account for future researches, are discussed in Section 8.

2. Panel-Based Potential Fields

As mentioned in the previous section, there are a handful of different approaches with various advantages and disadvantages for the definition of APFs. In the mean time, panel-based APFs could

https://doi.org/10.1017/S0263574714002100 Published online by Cambridge University Press

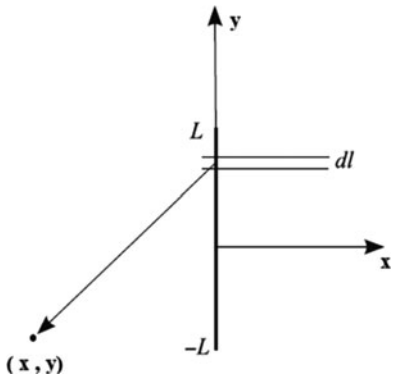

Fig. 1. Realization of panel.

be considered as robust options to be used in the navigation process due to modular property ascribed to the potential of obstacles and reliable reaction against local minima points.

A 2D panel, borrowed from hydrodynamics, could be considered as a vertical line along the height of the obstacle which is responsible for producing a repulsive potential all around the obstacle. The most indispensible property of the panel-based potentials is fulfilling the Laplace differential equation, i.e., utilization of this potential type can guarantee the resolving of the local minima problem intrinsically. Each panel could be known with two properties: the strength factor, and the height, which could be defined by Eq. (1), and could be studied in detail in ref. [26].[26] It deserves to stress that the height value is determined to prepare the desired integration bounds for Eq. (2). This value could be initialized with the height of the obstacle, which the panel is dedicated to. The other computationally efficient option could be any multiplication of the height of the obstacle. In the rest of this paper, the former approach will be taken into account,

$$\phi = \frac{\lambda}{2\pi} \ln r, \tag{1}$$

where λ is the strength factor of source ($\lambda < 0$) or sink ($\lambda > 0$) potential, and r is the range between the desired point and the panel. Potential integration along the panel, as shown in Fig. 1, will be culminated in reaching the potential according to the seminal elements of surface as in Eq. (2),

$$\phi = \frac{\lambda}{4\pi} \int_{-L}^{L} \ln\left(x^2 + (y - l)^2\right) \mathrm{dl}, \tag{2}$$

where ϕ represents the result of the potential.

As shown in Fig. 1, L stands for the half-length of the panel, on which the integration could be defined. One could imply that the symmetric placement of panel in the utilized coordination is due to the acquisition of more flexibility to anticipate the computational behavior of integrated potential.

Attenuating variation of ϕ, as depicted in Fig. 2, shows the efficient resolving of local minima points.

In view of practical implementation, an appropriate mapping should be utilized to transform acquired potentials into applicable parameters to robot's locomotion system. Such parameters could be evaluated as robot velocity according to each element of surface, as illustrated by below given equations:

$$V_1(x, y) = -\frac{\partial \phi}{\partial x} = \frac{-\lambda}{2\pi}\left(\arctan\frac{y + L}{x} - \arctan\frac{y - L}{x}\right), \tag{3}$$

$$V_2(x, y) = -\frac{\partial \phi}{\partial y} = \frac{-\lambda}{4\pi} \ln\left(\frac{x^2 + (y + L)^2}{x^2 + (y - L)^2}\right). \tag{4}$$

https://doi.org/10.1017/S0263574714002100 Published online by Cambridge University Press

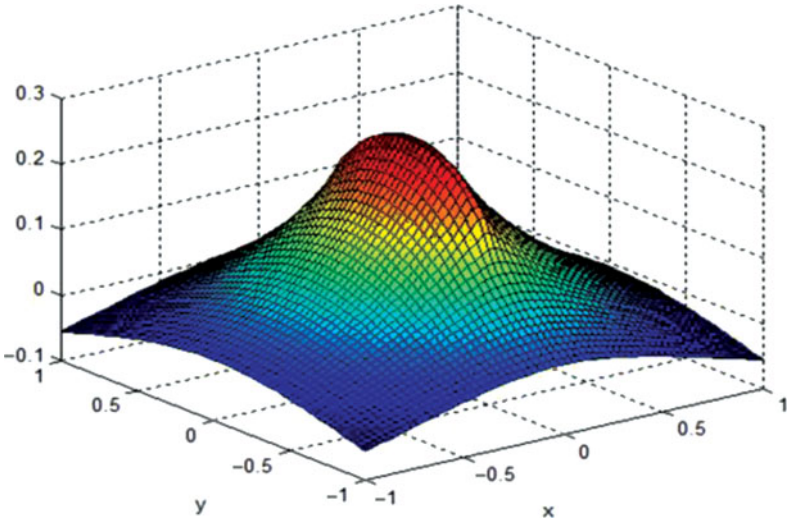

Fig. 2. Variation of the panel-based potential.

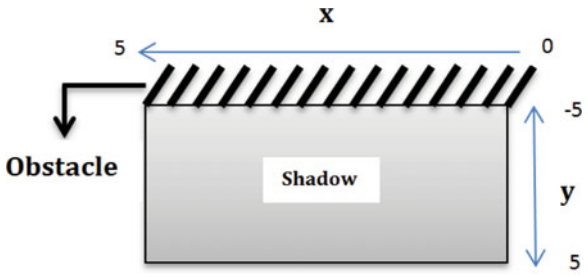

Fig. 3. A typical rectangular shadow.

Interested reader could trace the extraction of above equations in detail in ref. [26]. It is worth to verify the variation of acquired velocities for a typical shadow similar to the rectangular one, as shown in Fig. 3. Upper hatched area acts as an obstacle.

Considering assumed measures of the aforementioned figure, robot's velocity corresponding to each point in the circumferential terrain of obstacle will be acquired by the utilization of Eqs. (3) and (4) and could be depicted as in Figs. 4 and 5, which are utilized to illustrate the velocity corresponding to x and y directions.

Gratifying variation of the gained velocity along both directions may confirm the validation of utilized mapping from the potential space to the velocity space. As shown in both Figs. 4 and 5, velocities chose their own minimum values.

3. Mathematical Structure of TAPF

Shadow is a time-variant phenomenon that depends on some parameters of terrain and source of light, such as width and height of obstacles, quantitative variation of shadow around the obstacle, shape of the shadow, and so on. Therefore, it is reasonable to commence investigation on the invention of new APF with a special analysis of the behavior of the shadow around the obstacles, which could be either directional or longitudinal. Furthermore, consideration of distinctive potentials for obstacles and their shadows could lead to apply modularity properties regarding them. In this case, handling of generated potentials by obstacles and shadows will be independent and this could be known as an achievement in the management of APFs in the presence or absence of shadows. As a sequel, total potential, which will be applied to the navigation system, will be divided into two parts, as described by Eq. (5):

$$\phi = \phi_{\text{fix}} + \tilde{\phi}. \tag{5}$$

https://doi.org/10.1017/S0263574714002100 Published online by Cambridge University Press

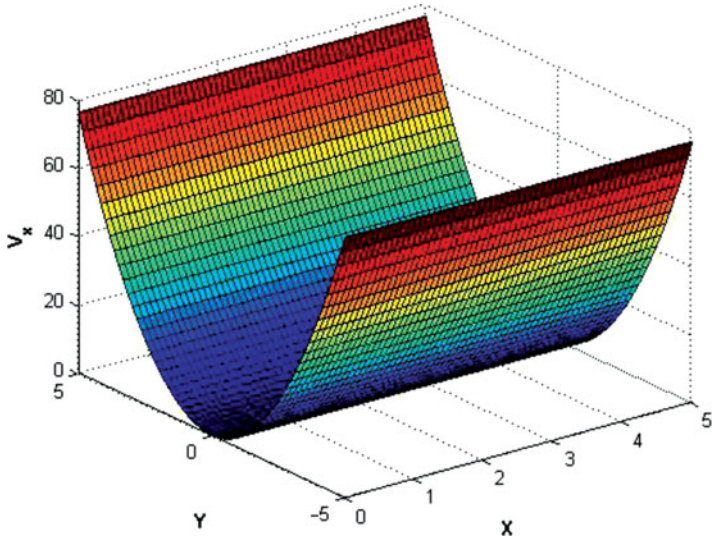

Fig. 4. Depiction of robot velocity along x-direction.

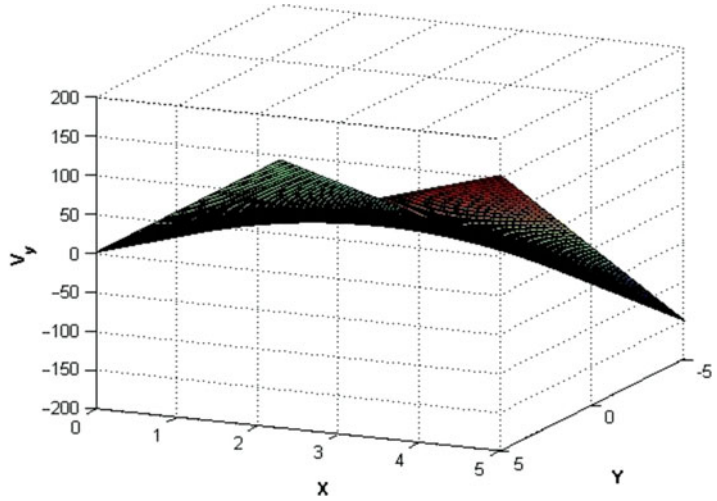

Fig. 5. Depiction of robot velocity along y-direction.

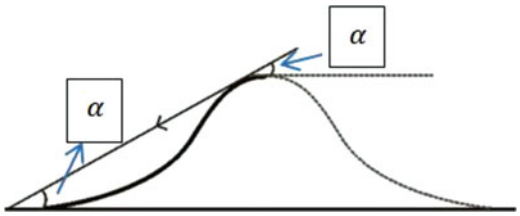

Fig. 6. A typical obstacle (x–z view).

Handling of obstacles will be done by ϕ_{fix} term, whereas mounting of $\tilde{\phi}$ term is due to the control of shadow potentials. Note that both of the aforementioned potential terms will be defined by the panel theory; but it is predictable that $\tilde{\phi}$ might be more complex because of its time-variant nature.

Considering the radiated light beam generated by the cosmetic light source of the assumed planet, shadow will be constructed on the other side of the obstacle (Fig. 6).

https://doi.org/10.1017/S0263574714002100 Published online by Cambridge University Press

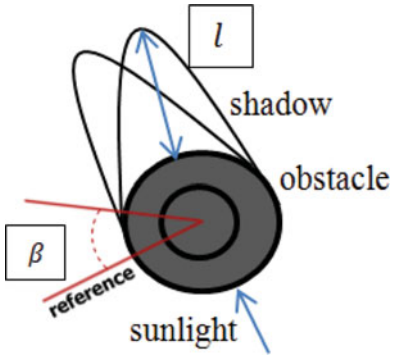

Fig. 7. A typical obstacle (x–y view).

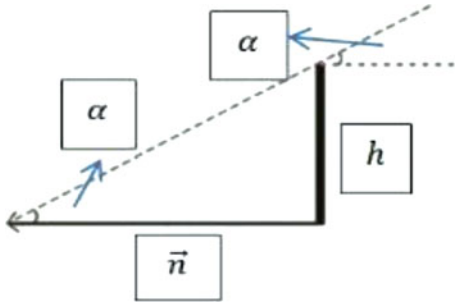

Fig. 8. The configuration of $\vec{n}$.

In Fig. 6, angle α is used to illustrate the angle of light beam in relation to the horizon. Angular motion of the shadow is synchronized with its longitudinal periodic variation with day and night. Shadow begins its rotation around the obstacle from sunrise to sunset, amounting to half of complete rotation. Also, length of the shadow varies noticeably within the mentioned time zone. Above points are succinctly depicted in Fig. 7.

Equation (6) shows the variation bound of introduced parameters in Fig. 7,

$$\begin{cases} l : [0, \infty) \\ \beta : [0, \pi] \end{cases}, \tag{6}$$

where l stands for the length of the shadow and β could be known as a quantitative explanation of the rotation of the shadow around the obstacle.

Taking a closer look at the shadow in the $(x - z)$ view like Fig. 6, as shown in Fig. 8, lets us describe the direction of the shadow by vector $\vec{n}$. As analyzed later, $\vec{n}$ could be considered as one of the two seminal parameters that takes part in the definition of TAPF, ($\tilde{\phi} \propto \vec{n}$). Height of the shadow is shown by parameter h.

With due attention to the rule of angular velocity of planet (ω) in variation of $\vec{n}$ and seminal geometric relationships stipulated by Fig. 5, Eqs. (7) and (8) could be acquired as mentioned below:

$$|\vec{n}| = \frac{h}{\tan \alpha}, \tag{7}$$

$$\vec{n} = \tan^{-1} \frac{n_y}{n_x} = \omega t. \tag{8}$$

Standard vector form of $\vec{n}$, as in Eq. (9), could be provided with simultaneous solution of above equations, which is explained by Eq. (10),

$$\vec{n} = n_x \hat{i} + n_y \hat{j}, \tag{9}$$

https://doi.org/10.1017/S0263574714002100 Published online by Cambridge University Press

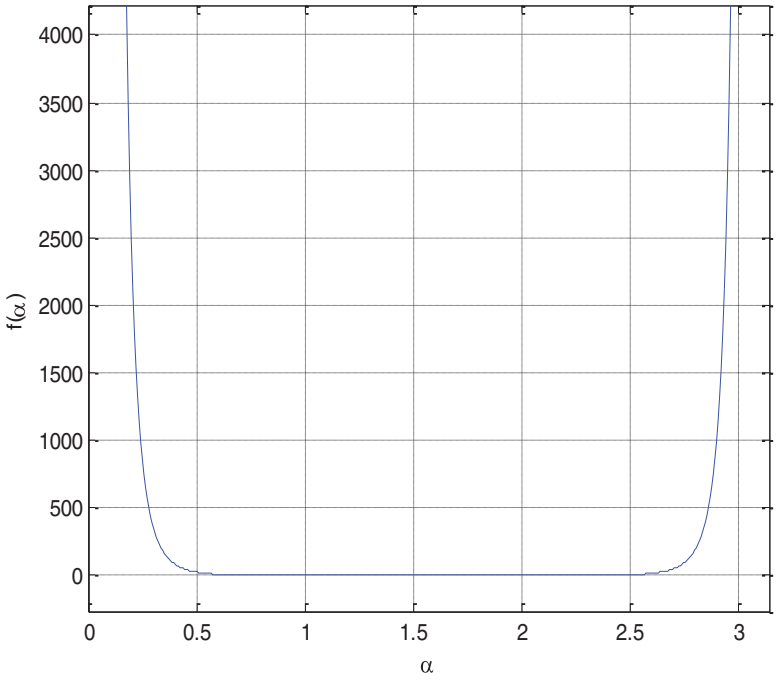

Fig. 9. Variation of $f(\alpha)$.

$$\vec{n} = \frac{h\,(\cos\omega t)^2}{\sin\omega t}\hat{i} + h\,|\cos\omega t|\,\hat{j}, \tag{10}$$

where $\hat{i}$ and $\hat{j}$ stand for the basic elements of 2D vector. It is worth noting that the height of each obstacle (h) will be assumed as the length of its corresponding panel in future analysis. Strength factor is another element in the panel-based APFs, which must be taken into account for the definition of TAPF concept. This coefficient also should be capable of turning around the obstacle in order to acquire an appropriate direction regarding the shadow and configuration of $\vec{n}$. So proposed strength factor ($\vec{\lambda}$) might be defined as a seminal element to extract TAPFs, and it consists of one scalar and one vector part. Investigation of boundary-desired variations of $\vec{\lambda}$ reveals that scalar part of $\vec{\lambda}$ depends on the α angle, i.e., in sunrise and sunset, where $\alpha \to 0$ and $\alpha \to \pi$, and the length of the shadow is empirically infinite. In the case of such singular values for α, strength factor must tend to infinity, reasonably. Furthermore, in the mid-day, radiation of beam light is perpendicular to horizon, i.e., length of the shadow goes toward zero, and in the absence of shadow, $|\vec{\lambda}|$ tends to zero. Aforementioned denouements could be depicted mathematically as in Eq. (11), and graphically as in Fig. 9:

$$f\,(\alpha) = \left(\frac{\alpha - \frac{\pi}{2}}{\sin\alpha}\right)^4. \tag{11}$$

Acquired scalar function must be included in a bunch of vector terms to be able to rotate upon time variation and appropriate illustration of the final vector strength factor concerning the seminal elements of terrain, i.e., x and y. To this objective, considering the primary deviation of $\vec{n}$ as an angle such as θ_0, direction of the shadow concerning each moment will be computed by Eqs. (12) and (13):

$$\theta = \omega t, \tag{12}$$

$$R_{\theta+\theta_0} = R_{\omega t+\theta_0} = R_{\omega t}\Theta, \tag{13}$$

https://doi.org/10.1017/S0263574714002100 Published online by Cambridge University Press

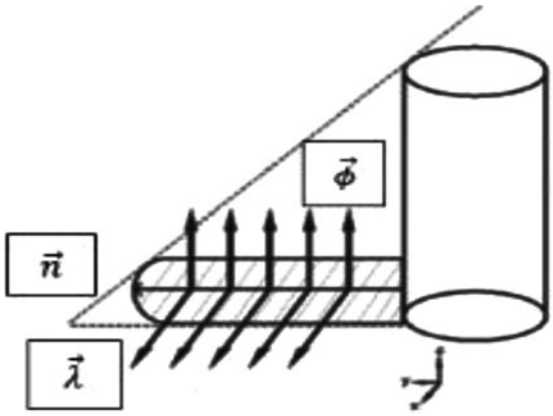

Fig. 10. Gaussian surface.

where ω is the angular velocity of the space mass and R_θ stands for the 2D rotation matrix, as shown in Eq. (14):

$$R_\theta = \begin{bmatrix} \cos\theta & -\sin\theta \\ \sin\theta & \cos\theta \end{bmatrix}. \tag{14}$$

As a sequel, vector strength factor for the panel of TAPF could be defined as given below:

$$\vec{\lambda} = \left(\frac{\omega t - \frac{\pi}{2}}{\sin \omega t} \right)^4 R_\theta \Theta \Lambda, \tag{15}$$

where Λ is used to enter the seminal elements, x and y, into the current notation,

$$\Lambda = \begin{bmatrix} x \\ y \end{bmatrix}. \tag{16}$$

The final touch in the definition of TAPF concept is the consideration of shadow surface as a Gaussian surface. Assuming the Gaussian surface, cross product of $\vec{n}$ and $\vec{\lambda}$ could be interpreted as a flux crossing that surface, whereas shadow is completely surrounded by the aforementioned vectors. Therefore, TAPF will be demonstrated by Eq. (17):

$$\tilde{\phi} = \oiint_S \left| \vec{n} \times \vec{\lambda} \right| d\sigma, \tag{17}$$

where $d\sigma$ is the differential surface element of terrain. The realization of Gaussian surface in addition to positions of $\vec{n}$ and $\vec{\lambda}$ is shown in Fig. 10.

with due attention to the noticeable computational complexity of the proposed equation for the computation of TAPFs, one may claim that utilization of powerful processors or decreasing the rate of sampling from TAPF is essential to handle the planning process and inhibition from the deadlock in computations. Section 5 is completely dedicated to notify some schemes to resolve such serious operational problems.

4. Control Architecture for Efficient Navigation

As previously stated, modular attitude toward potential effect of obstacles and shadows leads to apply different strategies in order to handle them individually. For providing multilateral control upon final applied artificial potential field to the locomotion system and the optimization of TAPF computation due to its computational complexity, a closed-loop control system consisting of some processing operators is taken onto account, as in Fig. 11. We are prone to present complete assertions upon the

https://doi.org/10.1017/S0263574714002100 Published online by Cambridge University Press

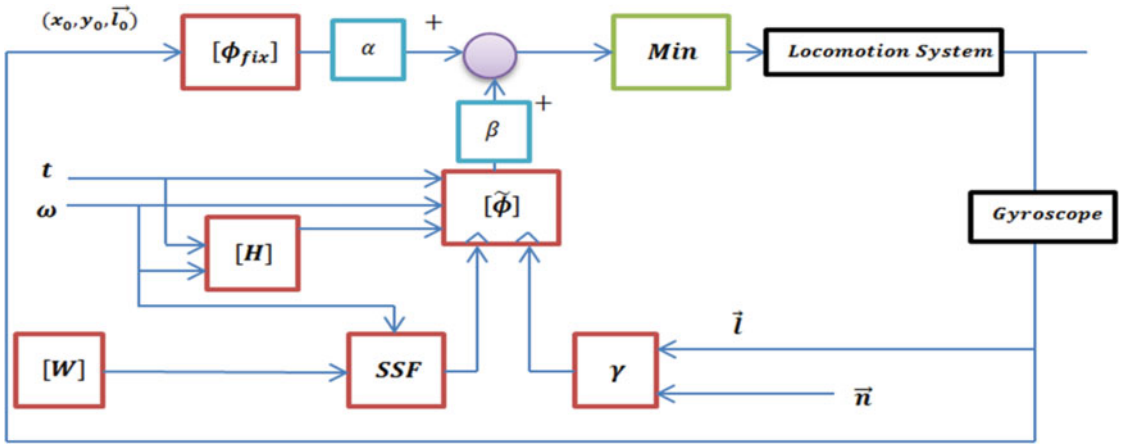

Fig. 11. Closed-loop architecture for the control of navigation problem.

mechanism of the named architecture and its subsequent blocks. As a matter of fact, each block is responsible for either the computation of a parameter or activation of a potentially inactive signal corresponding to other computational block.

Static APFs, which are referred to the potentials of obstacles, will be computed by ϕ_{fix} block, whereas $\tilde{\phi}$ block is turned to account for the calculation of TAPFs corresponding to shadows. Acquisition of both APF and TAPF allows the planner compute a linear combination of these as a total APF and minimize it in order to reach into the shortest path as Eq. (18),

$$\phi = \alpha\phi_{\text{fix}} + \beta\tilde{\phi}, \tag{18}$$

where α and β blocks could be considered as the factors that the designer may plan for interaction between APF and TAPF to achieve total APF. However, this factor strengthens the degrees of freedom to acquire more flexible values for total APF, achievement of the optimized total potential may seem critical. One may claim that Eq. (18) and the designer's capability of tuning α and β factors overshadow the optimality of the acquired route, which is generated by above navigation architecture. In the proposed scheme, it is the manifestation of a trade-off between gaining noticeable flexibility in distinguishing both behavior and probable priority of static or time-variant APFs and reaching into the globally optimized version of terrains in which the algorithm could be ended. In other words, there is a hierarchical relationship between global solution and suboptimal ones which are connected together by applying the proportional coefficients of Eq. (18). One might interpret the aforementioned equation as a superposition between static APF and TAPF, which is mounted to tract the effect of virtual potential of TAPF versus real potential of obstacles, represented by static APF. Considering Eq. (2), inputs of the ϕ_{fix} block, as current direction of robot and its coordinate in the viewpoint of reference frame, could be predictable. *Gyroscope* block is a general caption for every probable transducer to acquire state variables of the system, i.e., coordination and direction of robot.

Another element of the proposed configuration is locomotion system block. A mathematical mapping from potential space to state variables of robot should be turned to account for applying commensurate control law to robot for motion acquisition. As aforementioned by Eqs. (3) and (4), the first-order partial derivative of the potential field regarding surface elements could be considered as a realization for control law as velocity of robot. State realization of either kinematic or dynamic model of robot could be utilized to reach into the final step of motion planning, i.e., traversing the terrain.

5. Optimization of Computational Complexity

Proposed time-variant artificial potential field, as described by Eq. (17), suffered from sophisticated mathematical operations, which must be evaluated. Cross production of two vectors must be integrated

https://doi.org/10.1017/S0263574714002100 Published online by Cambridge University Press

upon a probable irregular surface of shadow. The problem could get rougher while considering various TAPFs of obstacles in the robot scope, which must be handled simultaneously, in addition to the high desired rate of potential sampling for the acquisition of acceptable precision in the extraction of terrain. With due attention to other complicated stuffs, which processor of the robot may confront with, this challenging problem could be ameliorated for high-speed processors by turning some optimization strategies to account for.

As the first attempt, computation of TAPF is under the aegis of a rather precise estimation from the shape of the shadow to provide integration bounds for Eq. (17). Machine vision approaches, as a wide group of reliable techniques, could be used to determine the shapes, but their noticeable computational overhead onto the processor may be considered as a drawback for their utilization. As a sequel, it is worth to gain a relationship among TAPFs of different shadow shapes. In a simulated approach, TAPF is evaluated for three shadow shapes, assuming height of the obstacle as 4 m and the angle of the sunlight radiation as 45°. The denouements are depicted in Table I.

As shown in Table I, potential variation of typical different shapes is entirely similar, except the acquired bounds of variation. Therefore, transformation of different shapes with the multiplication of simple proportional factors into each graph might be more efficient than deducting strict and computationally complicated criteria to investigate the environment in order to detect the exact shadow shape. This reality is predictable because the shapes are only responsible for the determination of integration bounds and the seminal point in the potential variation solely depends on the constant kernel of integral.

The rest of the strategies, which are depicted in Fig. 8, are mounting of SSF and γ blocks. As another attitude toward computational optimization of TAPF idea, calculation of new TAPF sample may be taken into account when it differs considerably from the previous sample. If so, then the definition of a paragon for making decision about the threshold of difference could resolve the optimization stuff. According to the aforementioned points, SSF block is mounted to determine quantitative value as a frequency for avoiding excessive and useless computations of TAPF. Quantitative variation of some circumferential parameters should be taken into account to acquire a coherent effect on sampling process. High angular velocity of planet intrinsically increases the sampling rate due to probable fast changes not only in the shape but also in the direction of the shadow, which means planner must enhance SSF value. Furthermore, more the width the obstacle has, more trivial variation of the shadow exists. Therefore, definition of SSF paragon could be summarized mathematically by Eq. (20),

$$\begin{cases} (SSF)^{-1} \propto \omega \\ (SSF)^{-1} \propto w^{-1} \end{cases}, \tag{19}$$

$$(SSF)^{-1} = \omega \sum_{i=1}^{k} \frac{1}{w_i}. \tag{20}$$

Usual convergence of Eq. (20) to an acceptable span with increasing number of obstacles could be evaluated as an advantage. Considering noticeable size of obstacles on planets in relation to the size of space robots, approximation of w_i terms based on vision techniques could be acceptable in the estimation of SSF. As a sequel, the step-wise operation of sampling algorithm with tuning SSF parameter to account for could be described as a flowchart given in Fig. 12, in which the sampling process in the $(k+1)$th step is taken into account.

As shown in Fig. 12, computation of new TAPF is just allowed if SSF paragon is sufficed and total checking time is not over. Output of sampling process is used by navigation system.

The final touch for the intuitive computation of TAPF integral is the motivation for insertion of γ block into the navigation system. Obviously, location of robot regarding the obstacle and the orientation of shadow could be taken into account to decide for the occurrence of robot's entrance into the shadow. As a qualitative classification, robot may be located around the obstacle, as shown in Fig. 13.

Single large vector is used to show the direction of robot movement, whereas small ones show the probable directions of shadow around a typical obstacle. The robot will be trapped into shadow if the direction of shadow follows bold vectors in each configuration. It is the manifestation of necessity

https://doi.org/10.1017/S0263574714002100 Published online by Cambridge University Press

Table I. Similar variation depiction for different shapes of shadow.

Bound of variation	Graphical variation of TAPF	Shadow shape
[−350, 0]	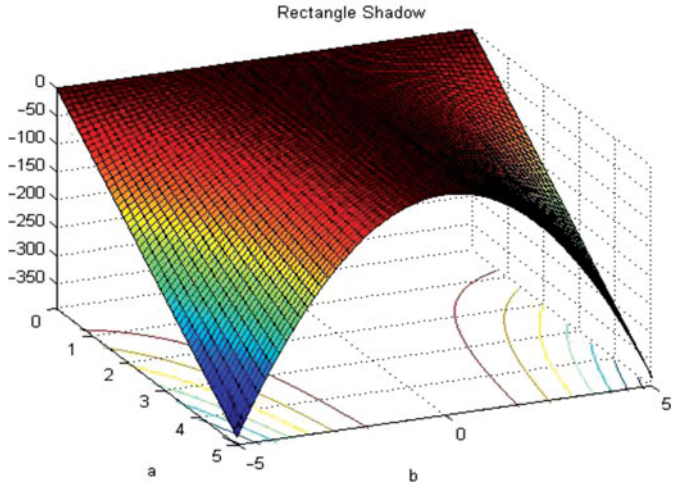	Rectangular
[−20000, 0]	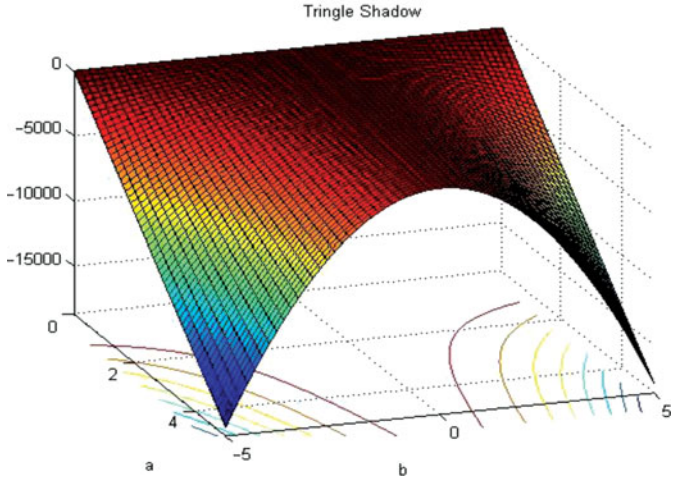	Triangular
[−12000, 0]	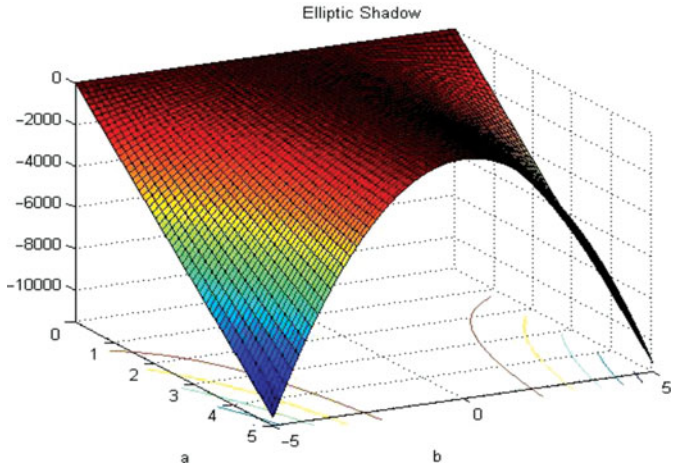	Elliptic

https://doi.org/10.1017/S0263574714002100 Published online by Cambridge University Press

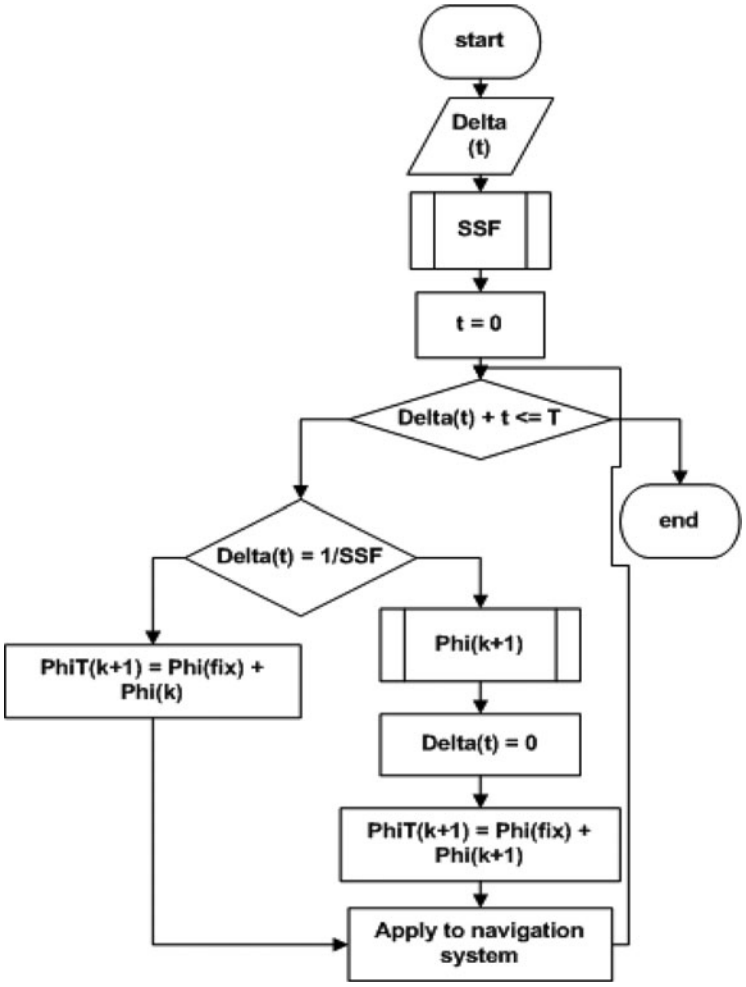

Fig. 12. Sampling architecture.

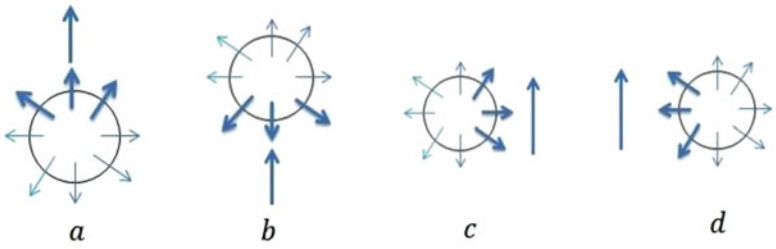

Fig. 13. Corresponding configuration of robot and obstacle.

for disabling TAPF computation when the robot does not confront with bold directions. In order to avoid the useless computation of potential field, some mathematical conditions could be acquired regarding the directions of both robot and shadow for different configurations given in Figs. 13a, b, c, and d as Eqs. (21)–(24) respectively:

$$\text{Fig13a} : \vec{n}.\vec{l} < 0, \tag{21}$$

$$\text{Fig.13b} : \vec{n}.\vec{l} \geq 0, \tag{22}$$

https://doi.org/10.1017/S0263574714002100 Published online by Cambridge University Press

Table II. Variables of a fuzzy controller.

	Variable description	Symbol
Inputs	Robot place related to obstacle	$Place$
	Deviation of vector $\vec{n}$	θ_n
	Deviation of vector $\vec{l}$	θ_l
Output	On-off state of block	γ

Table III. Approximate bound of variation for each variable.

Complete name	Symbol	Approximate bound of variation
VerySmall	VS	Around 0 or 360°
Small	S	Around 90°
Big	B	Around 180°
VeryBig	VB	Around 270°

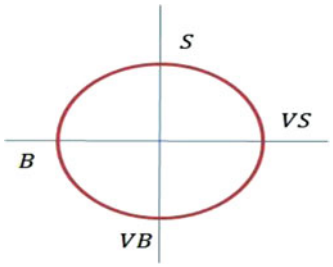

Fig. 14. Reference circle.

$$\text{Fig.13c}: \begin{cases} \theta_l - \theta_n < 0, \vec{n}.\vec{l} \geq 0 \\ \text{or} \\ \theta_l - \theta_n < 0,\ \vec{n}.\vec{l} < 0,\ \theta_l - \theta_{n+l} < 0 \end{cases}, \tag{23}$$

$$\text{Fig.13d}: \begin{cases} \theta_l - \theta_n > 0, \vec{n}.\vec{l} \geq 0 \\ \text{or} \\ \theta_l - \theta_n < 0,\ \vec{n}.\vec{l}\ \langle 0, \theta_l - \theta_{n+l} \rangle\ 0 \end{cases}, \tag{24}$$

where θ_n and θ_d represent the angles of $\vec{n}$ and $\vec{d}$ respectively regarding the base of trigonometric circle.

With due attention to the considerable intricacy of above equations, analytical decision-making about them certainly puts to question the primary reason of planning of γ block. Therefore, the implementation of smart approaches such as fuzzy control may lead to improve the overall efficiency of planning process. Based on the previous analysis, the classification of fuzzy inputs are shown as Table II.

Considering possible 360° deviation around each obstacle, the circumferential surface around the obstacle should be divided into some parts to be capable of defining membership functions for both θ_n and θ_l variables. Fig. 14 and Table III are used to illustrate the reference circle and approximate bound of variation for each membership function.

Precise values that are used in practical tests and are applied into the real system could be acquired as given below.

https://doi.org/10.1017/S0263574714002100 Published online by Cambridge University Press

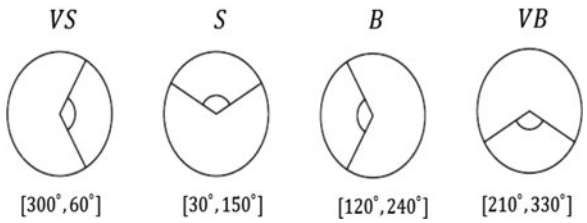

Fig. 15. Graphical bound determination of variables.

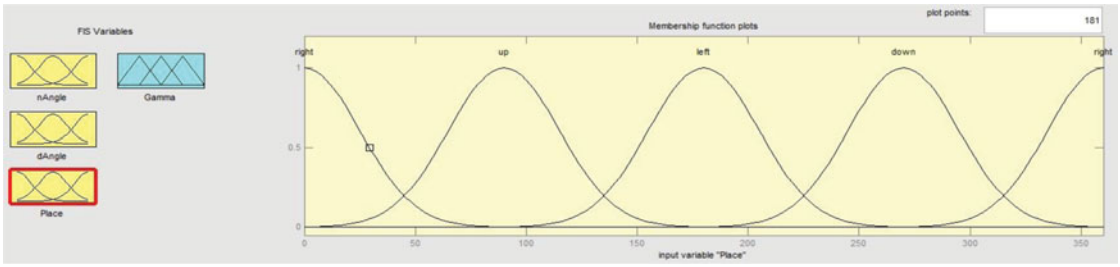

Fig. 16. Membership function for θ_n and θ_l.

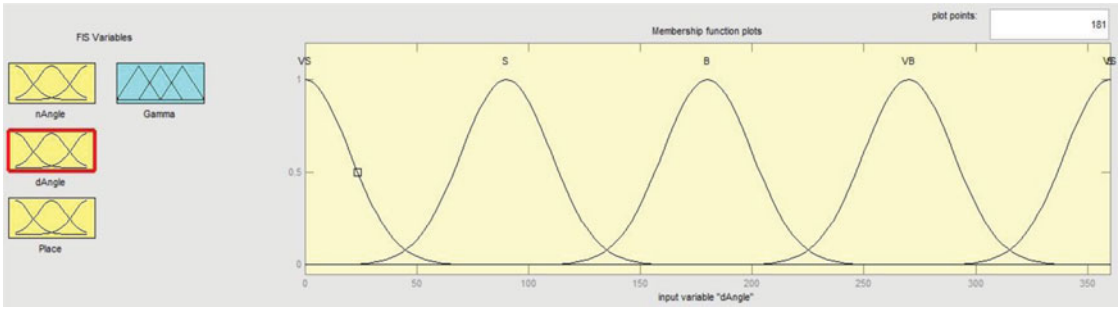

Fig. 17. Membership function for $Place$.

Turning similar membership function to account for both $\vec{n}$ and $\vec{l}$ vectors might be stipulated due to the same area traversed by them. In addition, $Place$ variable could be partitioned into four regions, as depicted in Fig. 13, to determine the relative location of robot and obstacle, i.e., regions will be labeled as up, $down$, $left$, and $right$. Guassian functions, due to their simple handling, are often taken into account for the variables with closed bounds. As a sequel, membership functions for the angles are determined by a typical Gaussian function, which is illustrated by Eq. (25):

$$f(v) = \frac{1}{\sqrt{40\pi}} e^{-\frac{(u-M)^2}{20}}, \tag{25}$$

where u $\in$ [0, 360] could act as the input angle of either $\vec{n}$ or $\vec{l}$ vectors. Furthermore, M stands for the mean factor. It is suffice to say that this parameter could be evaluated as a middle value for each deviation bound, as shown in Fig. 15. Obviously, the applied variance factor in the above equation is 20°, which should be considered to tract the variation of membership function. Similar strategy is taken into account for $Place$ variable, except that planned variance is equivalent to 30, which leads to smoother attitude toward transitions among regions regarding variations of θ_n and θ_l. Graphical realization of above variables is shown as Figs. 16 and 17.

Furthermore, output of the block should act like a switch. So applying Gaussian functions may sound inefficient reasonably, and its operation could be easily modeled by two sigmoidal membership

https://doi.org/10.1017/S0263574714002100 Published online by Cambridge University Press

Table IV. Activation fuzzy rules.

θ_n	θ_d	*Place*
VS	VS	$\downarrow\uparrow$
VS	S	$\downarrow\uparrow\rightarrow$
VS	B	$\rightarrow$
VS	VB	$\rightarrow$
S	VS	$\uparrow$
S	S	$\uparrow\leftarrow\rightarrow$
S	B	$\uparrow\leftarrow\rightarrow$
S	VB	
B	VS	$\leftarrow$
B	S	$\downarrow\uparrow\leftarrow$
B	B	$\downarrow\uparrow\leftarrow$
B	VB	
VB	VS	$\downarrow$
VB	S	$\downarrow$
VB	B	$\downarrow\leftarrow\rightarrow$
VB	VB	$\leftarrow\rightarrow$

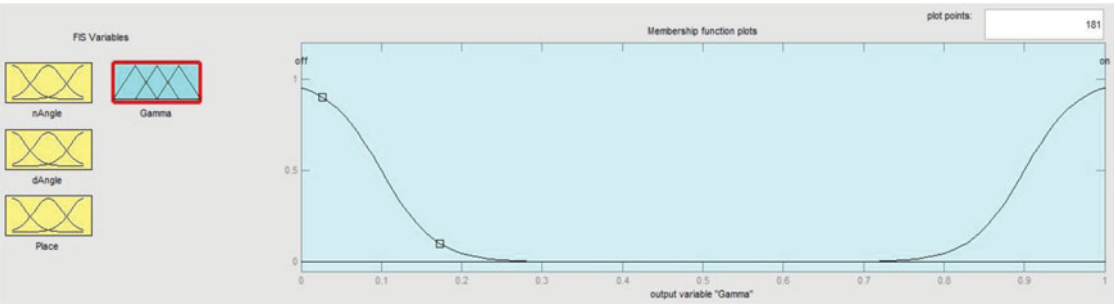

Fig. 18. Membership function for γ.

functions as Eqs. (26) and (27):

$$f_{\text{on}}(v) = \frac{1}{1 + e^{-30(v-0.9)}}, \tag{26}$$

$$f_{\text{off}}(v) = \frac{1}{1 + e^{30(v-0.1)}}, \tag{27}$$

where v $\in$ [0, 1].

Output depiction could also be shown as in Fig. 18.

Exploitations of fuzzy responses corresponding to Eqs. (21)–(24) will lead to complete the knowledge base of fuzzy system with desired variations of fuzzy variables to activate or deactivate the output of γ block. Investigation on these relationships reveals 28 fuzzy rules for activation and 28 fuzzy rules for its deactivation, where activation states are given in Table IV.

6. Extraction of Environmental Parameters

A short sight on the proposed control architecture, introduced in Section 4, reveals that some environmental information must be provided and fed into the operational blocks of the controller to reach the desired functionality of the navigation system. As a sequel, determination of width and height of obstacles, in addition to the detection of angle of light radiation, could be considered as the parameters that should be determined within the navigation process. One may postulate that machine vision techniques, such as stereo vision and visual odometry, are able to resolve the extraction problem easily. But with due attention to the non-trivial computational complexity of the mentioned algorithms

https://doi.org/10.1017/S0263574714002100 Published online by Cambridge University Press

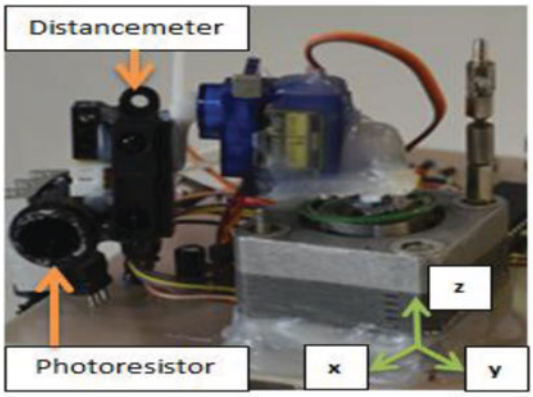

Fig. 19. Mounted set of sensors and actuators.

Fig. 20. Assembled photo-resistor package.

and all the arguments about the struggles for decreasing the forced computational overhead to the main processor of the robot mentioned in Section 5, it is better to apply more light schemes to aim the goal.

Obviously, the robot may need to survey its spatial circumference to exploit three seminal parameters. A distance meter module, such as *SHARPGP2D*12, is turned to account for presented experiments. Establishment of a 2D map from the environment by the aforementioned module could be planned as the first step in the survey, because not only the construction of the static APFs is entirely beholden to know the place of each obstacle but the base of the shadows just could be known with access to the center coordinate of the corresponding obstacles. Therefore, it sounds that a complete rotation around the z-axis should be taken into account for the distance meter module. Launching the current detection system leads to acquire both 2D map and width of obstacles, i.e., the radiation of module toward straight direction will accompany the reflection of the sent wave. In the absence of the obstacle in front of module, there will be no reflected wave. Considering the known frequency of the radiated wave, in addition to the angular velocity of module within the rotation, width of obstacles could be acquired. Utilization of a photo-resistor package may be commensurate to extract the sunlight direction. So, module and photo resistor must be able to traverse along the z-axis in order to determine the height of obstacles and detect the direction of sunlight. The suggested configuration for the above scenario is given in Figs. 19 and 20.

A stepper motor is also responsible for covering the rotation around the z-axis. Mounting a servo motor to the shaft of the stepper motor leads to reach into the complete spatial traversing of circumferential environment. As a last step, both distance meter module and photo resistor will be connected to the shaft of servo motor. Assumed spatial Cartesian coordinate is shown in Fig. 19. Denouements of the aforementioned approaches will be analyzed in detail in Section 7.

https://doi.org/10.1017/S0263574714002100 Published online by Cambridge University Press

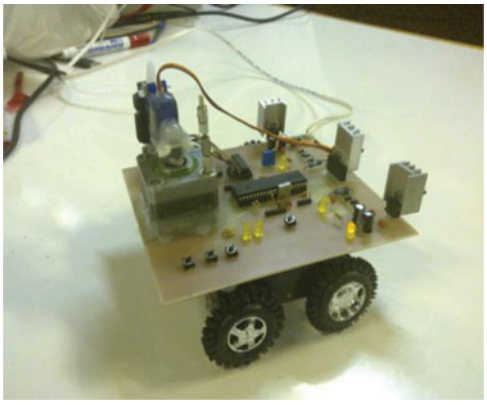

Fig. 21. PIONEER^{TM} mobile robot.

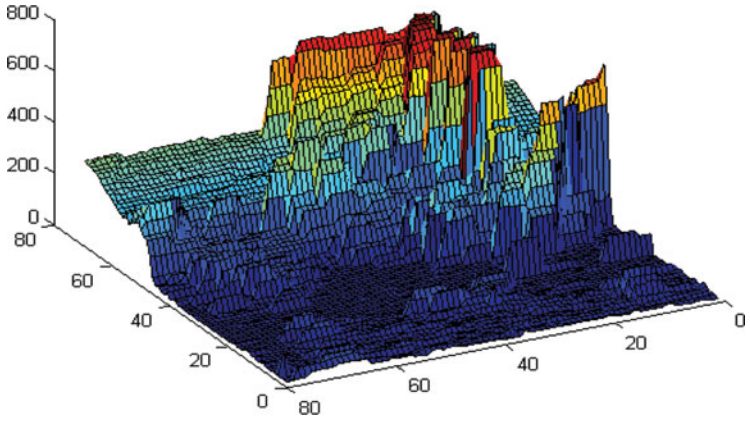

Fig. 22. Cartesian depiction of 2D circumferential scan.

7. Simulated Denouements and Practical Implementations

Practical implementation of the whole discussed designs in previous sections sounds necessary to evaluate the operational efficiency of the TAPF idea in the navigation of autonomous space robots in the presence of a shadow. To reach the mentioned objective, numerical data received from both sensors, i.e., distance meter module and photo resistor, must be construed. Variation of the aforementioned parameters should culminate in a reasonable perception from the environment. As a next step, APF and TAPF will be constructed by this verified data and the process of navigation could be assessed by the exertion of acquired potential fields on robot's locomotion system. As a test bed, PIONEER^{TM} mobile robot, as shown in Fig. 21, is manufactured to sample the environment and examine the quality and capability of planner system in the navigation process.

A typical 2D scan of the laboratory environment to acquire both map from the terrain in the vicinity of the robot and the detection of the width of obstacles is depicted as Figs. 22 and 23. Received raw data from scanning of the environment by planned rotation of distance meter module leads to Fig. 22, whereas the transformation of coordinate into spherical one might lead to a more coherent interpretation from variations, as given by Fig. 23. In such a condition, the distance meter module could be imagined completely in the center of the scanned sphere. With due attention to incomplete scan of the spatial environment because of imperfect rotations of motor set, acquired cut slice in the resulted sphere could be legitimized. Upper regions of the scanned area, shown in dark blue color, are entirely located out of module's scope. It is the manifestation of no available information about the terrain accidents in such scopes. Transformation of color into lighter ones reveals the existence of obstacles. Red area could be known as the nearest obstacle to the robot.

Furthermore, detection of light was introduced as another important matter that must be investigated within the navigation process. Rotation of photo resistor will lead to acquire similar plots from the environment. Above the test field in the laboratory, there were three lamps with different ranges from

https://doi.org/10.1017/S0263574714002100 Published online by Cambridge University Press

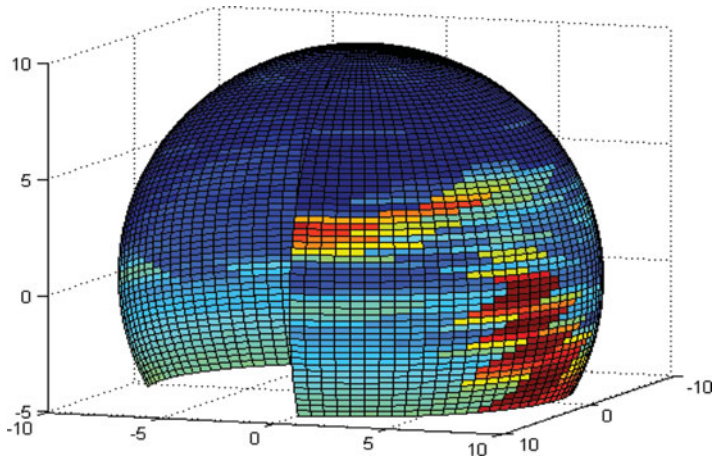

Fig. 23. Spatial depiction of 2D circumferential scan.

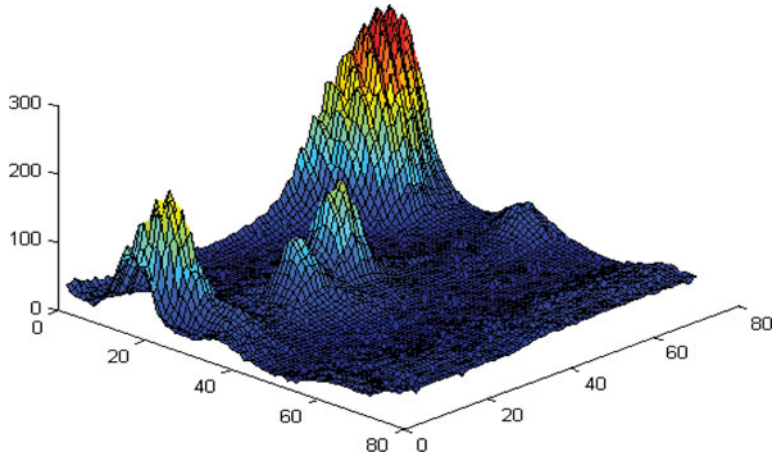

Fig. 24. 3D radiating scan in Cartesian coordinate.

the robot. In addition, sunlight was the other source of light for our rover. As a sequel, determination of mentioned sources must be gained by the results of photo-resistor traversing. Such results are shown in Figs. 24 and 25.

Interpretations of above figures are similar to Figs. 22 and 23. One may note noticeable small distance for one of the lamps above the robot. The biggest peak of the acquired surface, as shown in Fig. 24, could be construed as this light source. Smaller peaks might be referred to either the more far sources or weaker ones, whereas vast lighter regions on the spherical realization of the light scan, depicted in Fig. 25, provide the other attitude regarding the aforementioned perceptions. Furthermore, radiation pattern of light sources could be considered as the best tool for the detection of beam-light directions, which are given in Fig. 26.

As a final touch in the verification of navigation process and motion planning by TAPF, practical test of the navigation algorithm based on TAPF was taken into account and a typical terrain was considered to examine the ability of PIONEER^{TM} in path planning in presence of both obstacles and their shadows, as shown in Fig. 27.

The denouement of the above experiment and the generated potential field could be shown in Figs. 28 and 29 respectively.

Three typical obstacles are taken into account with different sizes and heights, which could be distinguished with dark blue shapes on trajectory plane, whereas white regions are turned to account for the representation of shadows. Source and target points are also determined. The experiment was executed twice. In the first run, the planner just utilized static APFs, i.e., no TAPF was take into account for obstacles. The light green trajectory, which is generated as a test result, is gratifying in

https://doi.org/10.1017/S0263574714002100 Published online by Cambridge University Press

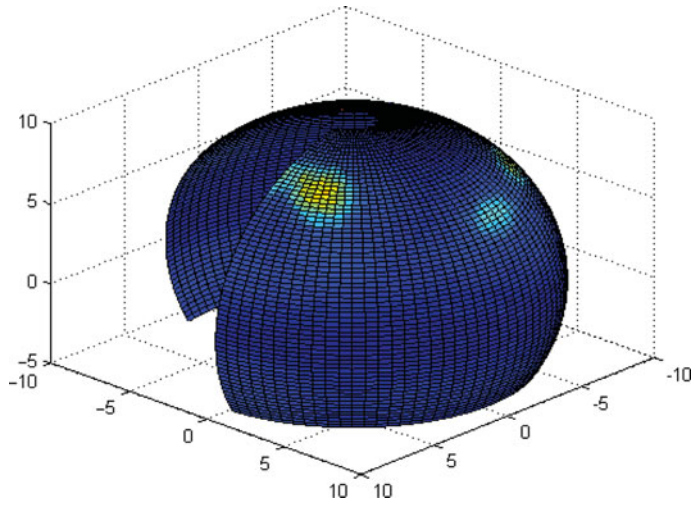

Fig. 25. 3D radiating scan in spherical coordinate.

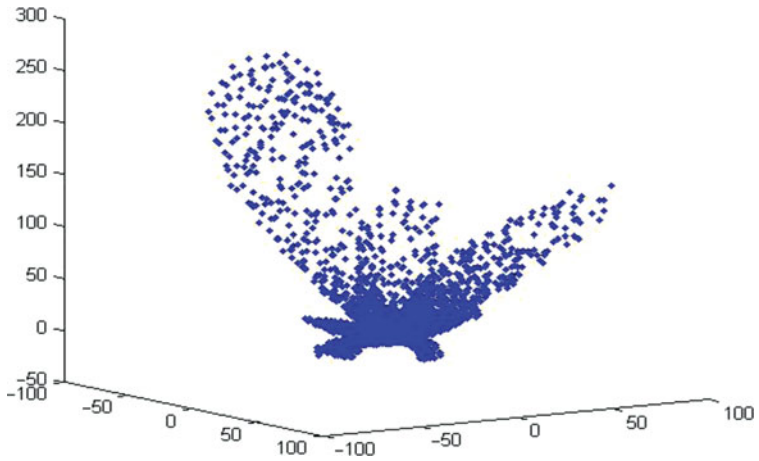

Fig. 26. Radiation pattern of light sources.

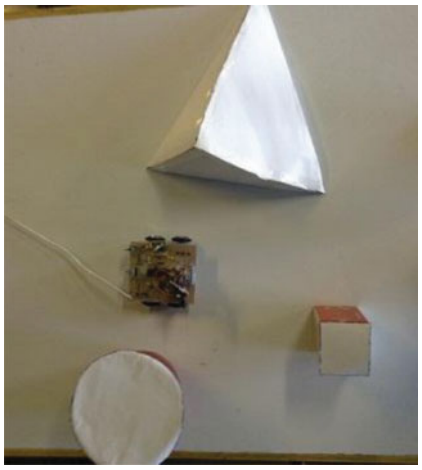

Fig. 27. A typical field.

https://doi.org/10.1017/S0263574714002100 Published online by Cambridge University Press

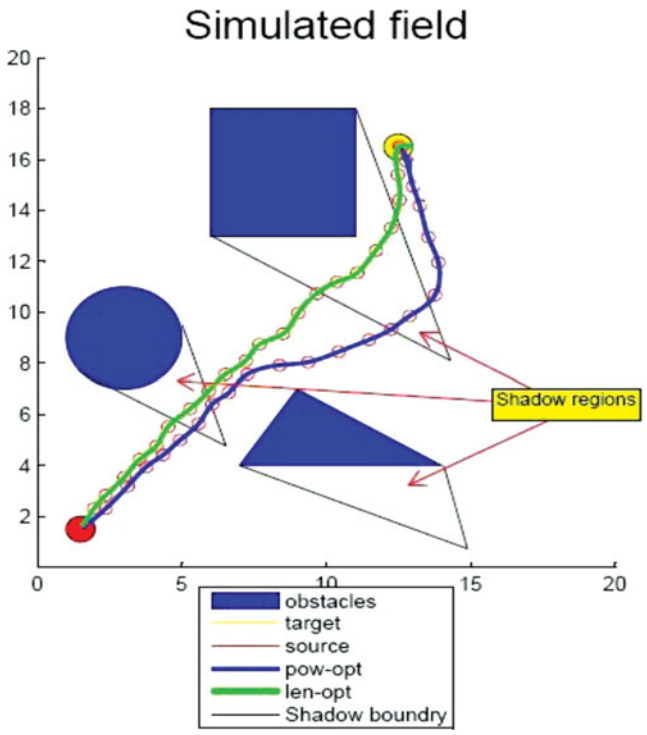

Fig. 28. Trajectory of PIONEER^{TM} within the test.

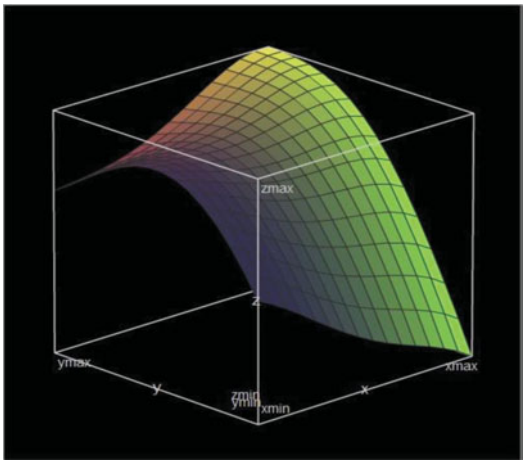

Fig. 29. Variation of potential for accomplished test.

view of the surveyed distance, but the depth of robot entrance into shadows is a drawback for such a strategy. As the second run, TAPFs are considered within the definition of potentials, in addition to custom APFs. As a sequel, the robot can detect shadow regions and contemplate them in the assessment of probable paths to reach the optimized one. Longer length of a new dark blue trajectory is undeniable in relation to the previous test, but the planner has succeeded to control the entrance depth into shadows as much as possible. It is worth to note that definition of the "optimized trajectory" may differ in view of the aforementioned experiments. On one hand, the first trajectory can guarantee the minimum traversed distance up to the target; however, it does not care about the management of the consummated power. So it is deserved to be called "length-optimized trajectory (L-OT)." On the other hand, second trajectory is the denouement of efficient turning of power resources to account for and maximization of the light power consumption in daily missions of planetary rover. Therefore, the light green path is qualified to be labeled as "power-optimized trajectory (P-OT)." Analysis of results

https://doi.org/10.1017/S0263574714002100 Published online by Cambridge University Press

Table V. Quantitative representation of achievements within empirical tests.

	Energy consumption (%)			
	Light (%)	Atomic batteries (%)	Elapsed time (insec)	Traversed distance (cm)
L-OT	65.3	34.7	43	72
P-OT	88.6	11.4	51	86

with different points of view by acquired quantitative parameters might be investigated to validate the presented approach, more reasonably, in Table V.

8. Concluding Remarks

In this research, TAPF is presented to acquire progressive planning process in some applications of mobile robotics, such as autonomous space rovers. Aforementioned approach is capable of modeling the state of shadow around each obstacle in the space field while considering a Gaussian surface corresponding to each shadow for the construction of virtual fluxes as TAPF realization. In addition, due to challenging computational complexity of the proposed scheme, some strategies are taken into account for efficient calculation of complicated integral of each TAPF. Different desired parameters, which are essential for the definition of TAPFs, lead to the consideration of a control architecture to reach into a coherent organized system for simultaneous handling of static APFs and TAPFs. Applied experiments to mentioned parameters show that utilization of machine vision techniques might be negligible, with due attention to both noticeable computational overhead for robot's central processor and appropriate achievements of mounted strategies to resolve the parameter extraction problem.

Furthermore, interaction coefficients between static APFs and TAPFs could be tuned by designer's opinion. Determination of those parameters may sound as a trade-off for acquiring a combined optimized path consisting of L-OT and P-OT. However, automaton of the aforementioned regulation could be considered as a key point for reaching into the next generation of control architectures under aegis of future researches. However, this research just tried to depict the validation of the proposed idea. Substitution of applied detectors with more modern equipment could provide appropriate opportunity to evaluate the capability of the presented strategy in real situations with specialized equipment. The empirical denouements completely verified the efficiency of the proposed TAPF in detection and handling of shadows within navigation process in space exploration missions.

References

1. S. Koenig and M. Likhachev, "Incremental A*," *Proceedings of the Neural Information Processing Systems* (2002) pp. 1539–1546.
2. A. Stents, "Optimal and Efficient Path Planning for Partially Known Environments,"**In**: *Proceedings of the IEEE International Conference on Robotics and Automation* (1994) pp. 3310–3317.
3. S. Koenig and M. Likhachev, "D* Lite," *Proceedings of the National Conference on Artificial Intelligence (AAAI)* (2002).
4. A. Stents, "The Focussed D* Algorithm for Real-Time Replanning," **In**: *Proceedings of the International Joint Conference on Artificial Intelligence* (1995) pp. 1625–1659.
5. J. Carsten, D. Ferguson and A. Stentz, "3D Field D: Improved Path Planning and Replanning in Three Dimensions,"**In**: *Proceedings of the IEEE/RSJ International Conference on Intelligent Robots and Systems* (2006) pp. 3381–3386.
6. M. Dakulovic and I. Petrovic, "Two-way D^* for path planning and replacing," *Robot. Auton. Syst.* **52**, 329–342 (2011).
7. O. Khatib, "Real-time obstacle avoidance for manipulators and mobile robots," *Int. J. Robot. Res.* **5**(1), 90–98 (1986).
8. J. Sfeir *et al.*, "An Improved Artificial Potential Field Approach to Real-Time Mobile Robot Path Planning in an Unknown Environment,"**In**: *Proceedings of the IEEE International Symposium on Robotic and Sensors Environments (ROSE)*, Canada (2011) pp. 208–2013.
9. S. S. Ge and Y. J. Cui, "Dynamic motion planning for mobile robots using potential field method," *Auton. Robot.* **13**(3), 207–222 (2002).
10. L. Huang, "Velocity planning for a mobile robot to track a moving target – a potential field approach," *Robot. Auton. Syst.* **57**, 55–63 (2009).

https://doi.org/10.1017/S0263574714002100 Published online by Cambridge University Press

11. D. Yagnik *et al.*, "Motion Planning for Multi-Link Robots Using Artificial Potential Fields and Modified Simulated Annealing," **In**: *Proceedings of the IEEE/ASME International Conference on Mechatronics and Embedded Systems and Applications (MESA)*, Canada (2010) pp. 421–427.
12. H. Mekki and M. Chtourou, "Variable Structure Neural Networks for Online Identification of Continuous-Time Dynamical Systems Using Evolutionary Artificial Potential Fields," **In**: *Proceedings of the 9th International Multi-Conference on Systems, Signals and Devices (SSD)*, Tunisia (2012) pp. 1–6.
13. Z. Hong *et al.*, "The Dynamic Path Planning Research for Mobile Robot Based on Artificial Potential Field," **In**: *Proceedings of the International Conference on Consumer Electronics, Communications and Networks (CECNet)* China (2011) pp. 2736–2739.
14. S. R. Munasinghe, C. Oh, J.-J. Lee and O. Khatib, "Obstacle Avoidance Using Velocity Dipole Field Method," *Proceedings of the International Conference on Control, Automation, and Systems (ICCAS)*, Korea (2005).
15. T. Zhang, Y. Zhu and J. Song, "Real-time motion planning for mobile robots by means of artificial potential field method in unknown environment," *Ind. Robot.* **37**(4), 384–400 (2010).
16. H. Bing *et al.*, "A Route Planning Method Based on Improved Artificial Potential Field Algorithm," **In**: *Proceedings of the 3rd IEEE International Conference on Communication Software and Networks (ICCSN)*, China (2011) pp. 550–545.
17. Q. Li *et al.*, "An Improved Artificial Potential Field Method for Solving Local Minimum Problem," **In**: *Proceedings of the 2nd International Conference on Intelligent Control and Information Processing (ICICIP)*, China (2011) pp. 420–424.
18. P. Vadakkepat, K. C. Tan and M. L. Wang, "Evolutionary Artificial Potential Fields and Their Application in Real Time Robot Path Planning," **In**: *Proceedings of the Congress on Evolutionary Computation* (2000) pp. 256–263.
19. M. Zhang *et al.*, "Dynamic Artificial Potential Field Based Multi-Robot Formation Control," **In**: *Proceedings of the IEEE Conference on Instrumentation and Measurement Technology (I2MTC)*, China (2010) pp.1530–1534.
20. P. Fiorini and Z. Shiller, "Motion Planning in Dynamic Environments Using the Relative Velocity Paradigm," **In**: *Proceedings of the IEEE/RSJ International Workshop on Intelligent Robot and Systems* (1993) pp. 560–565.
21. P. Fiorini and Z. Shiller, "Motion planning in dynamic environments using velocity obstacles," *Int. J. Robot. Res.* **17**(17), 760–772 (1998).
22. L. Guan-chen *et al.*, "Artificial Potential Field-Based Receding Horizon Control for Path Planning," **In**: *Proceedings of the 24th Chinese Control and Decision Conference (CCDC)*, China (2012) pp. 3665–3669.
23. L. Xiang *et al.*, "An Artificial Potential Field Model with Constraints," **In**: *Proceedings of the 31st Chinese Control Conference (CCC)*, China (2012), pp. 4680–4683.
24. H. Rezaee and F. Abdollahi, "Adaptive Artificial Potential Field Approach for Obstacle Avoidance of Unmanned Aircrafts," **In**: *Proceedings of the IEEE/ASME Internatonal Conference on Advanced Intelligent Mechatronics (AIM)*, Iran (2012), pp. 1–6.
25. C. Bentes and O. Saotome, "Dynamic Swarm Formation with Potential Fields and A* Path Planning in 3D Environment," **In**: *Proceedings of the Robotics Symposium and Latin American Robotics Symposium (SBR-LARS)*, Brazil (2012), pp. 74–78.
26. F. Fahimi, *Autonomous Robots Modeling, Path Planning, and Control* (Springer, Berlin, Germany, 2009), pp. 88–92.
27. M. Macktoobian and S. A. A. Moosavian, "Time-Variant Artificial Potential Fields: A New Power-Saving Strategy for Navigation of Autonomous Mobile Robots," **In**: *Proceedings of the 1st RSI/ISM International Conference on Robotics and Mechatronics (ICRoM)*, Iran (2013), pp. 121–127.
28. M. Macktoobian, "Smart Navigation of Smart Mobile Robots by Time-Variant Artificial Potential Fields," *Proceedings of Iranian Conference on Fuzzy Systems (IFSC)*, Iran (2013) pp. 1–6.